Group members：Shengzhuo Wang, Chenxu Hu, Shixing Yu

School：Tsinghua University High School

Province：Beijing

Country/Region：China

Instructor：Xinfu Chen

Title：Synthesis of the PEG-PLGA-coated Fe_3O_4 nanoparticles by double-emulsion method

Contents

Title: Synthesis of the PEG-PLGA-coated Fe_3O_4 nanoparticles by double-emulsion method .4

Abstract 4

1 Introduction 8

2 Experiments 12

2.1 Materials 12

2.2 Synthesis of chitosan quaternary ammonium salt Fe_3O_4 nanoparticles ...12

2.3 Characterization of nanoparticles 17

2.4 Cell experiment 18

3 Results and discussion 19

3.1 Transmission electron microscopy analysis 19

3.2 Particle size analysis of nanoparticles 20

3.3 Analysis of fourier transform infrared spectra 21

3.4 X-ray diffraction analysis 23

3.5 Analysis of hysteresis loop 24

3.6 Analysis of zeta potential 25

3.7 Analysis of relaxation rate 26

3.8 Determination of entrapment efficiency and loading content 29

3.9 Cell experiments results 30

4 Conclusion 31

References 33

Acknowledgments 37

Resumes of the team members and instructor 38

List of Figures

Fig. 1 Experimental apparatus

Fig. 2 Preparation of Fe_3O_4@CSQ nanoparticles

Fig. 3 Fe_3O_4@CSQ nanoparticles encapsulated by double emulsion method

Fig. 4 TEM images of Fe_3O_4@CSQ, PEG-PLGA, and Fe_3O_4@CSQ-PEG-PLGA

Fig. 5 Particle size distribution curves

Fig. 6 FTIR of the polymers and the products

Fig. 7 X-ray diffraction of the synthesized Fe_3O_4

Fig. 8 Hysteresis loop of Fe_3O_4@CSQ and Fe_3O_4@CSQ-PEG-PLGA

Fig. 9 Zeta potential

Fig. 10 The relaxation rate of MRI-T_2 and MRI-T_1

Fig. 11 The relaxation rate of Fe_3O_4@CSQ and Fe_3O_4@CSQ-PEG-PLGA

Fig. 12 The relationship between Fe_3O_4 encapsulate efficiency (EE) and loading content (LC) and the ratio of Fe_3O_4 to PEG-PLGA

Fig. 13 The Cell viability of Fe_3O_4@CSQ-PEG-PLGA (a) and Fe_3O_4@CSQ (b)

Title: Synthesis of the PEG-PLGA-coated Fe_3O_4 nanoparticles by double-emulsion method

Abstract

Magnetic resonance imaging (MRI) is often used with transition metals and other paramagnetic substances (such as iron, gadolinium, nickel, etc.) as a paramagnetic contrast agent. Compared to other metals, the ferroferric oxides (Fe_3O_4) have higher biocompatibility and have aroused great attention. Fe_3O_4 nanoparticles show superparamagnetism and magnetic tunneling effect and have quantum effect and large specific surface area. It has good contrast effect, and has been studied as high efficient T_2 contrast agents.

The chitosan quaternary ammonium salts (CSQ) is a cationic polymer electrolyte, containing hydrophilic groups, good biocompatibility, and good biodegradability, so they are widely used in drug loading, releasing, and controlling, and preparation of antibacterial biomaterials. As chitosan quaternary ammonium salt is the surface ligand of Fe_3O_4 nanoparticles, the positive charge is very strong, so they can be reunited in the negative charged blood, resulting in fatal thrombus and hemolysis to human.

Polyethylene glycol and polylactic acid-glycolic acid copolymer (PEG-PLGA) is a biocompatible, biodegradable amphiphilic polymer material. Use of PEG and PLGA as drug carrier system has been reported that the release of the drugs can be controlled and they can protect the activity of the drug better. PEG-PLGA has no obvious immune response and cytotoxicity, and the biosafety is very high.

Based on the research background above, in order to find a relatively safe and reliable ferroferric oxide (Fe_3O_4) contrast agent, the Fe_3O_4@CSQ nanoparticles were prepared by coprecipitation method, and then, being placed in polyvinyl alcohol (PVA), polyoxyethylene-polyoxypropylene block copolymers (F68) (here PVA and F68 as emulsion stabilizer), coated PEG-PLGA twice to get the Fe_3O_4@CSQ-PEG-PLGA nanoparticles. Therefore, the nanoparticles using PEG as surface which has good

hydrophilicity can circulate *in vivo* for long time.

The results of electron microscopy and particle size analysis showed that the aggregation and growth of Fe_3O_4 crystallites were limited by the surface coated CSQ, and the magnetic composite particles were obtained. Their particle size is small and uniform. According to FTIR spectrometry and X-ray powder diffraction characterization, the existence of Fe_3O_4 in the nanoparticles was confirmed and PEG-PLGA has better effect while coating Fe_3O_4@CSQ. According to the analysis of correlation properties, including the hysteresis loop, zeta potential, the relaxation and utilization rate of Fe_3O_4, the nanoparticles have small particle size, negative zeta potential (avoid the aggregation with negatively charged protein) and long circulation time in human body. At the same time, the nanoparticles were super-paramagnetic. Therefore, these features show that (in contrast to the lesion) Fe_3O_4@CSQ-PEG-PLGA nanoparticles will produce good imaging results. Use different mass ratio between Fe_3O_4@CSQ and PEG-PLGA to do the emulsification experiment, measure the entrapment efficiency and loading content respectively, and find the best ratio to use the materials most efficiently to provide guidance to future mass production of this kind of contrast agent.

In order to verify the biosafety of the prepared contrast agent, the cytotoxicity of Fe_3O_4@CSQ-PEG-PLGA was tested in this study. The results showed that the biosafety of Fe_3O_4@CSQ-PEG-PLGA nanoparticles significantly increased and there were almost no toxic side effects on cells.

The highlight of this research is the selection of biocompatible and biodegradability materials CSQ and PEG-PLGA, using double-emulsion method synthesis of PEG-PLGA coated Fe_3O_4 nanoparticles to prepare the magnetic material and improve the electrical properties. This Fe_3O_4 nanoparticles contrast agent is expected to solve the problem of the coagulating with negatively charged protein in the blood which causes thrombus and hemolysis.

Keywords: Iron oxide nanoparticles; Chitosan quaternary ammonium salts; PEG; PLGA; Double-emulsion method; Characterization

Statement of Originality

The research experiments and results of this team are conducted and derived under the guidance of the instructor. Other than the referenced content and the acknowledged sources, this paper does not include any published findings by this group or any other researchers. If there is any inaccuracy, this team is accountable for all liabilities.

Signature: Shengzhuo Wang, Chenxu Hu, Shixing Yu

ABBREVIATIONS

Abbreviation	Full name
MRI	Magnetic resonance imaging
CSQ	Chitosan quaternary ammonium salt
PEG-PLGA	Polyethylene glycol and polylactic-co-glycolic acid copolymer
PVA	Polyvinyl alcohol
F68	Polyoxyethylene-polyoxypropylene block copolymers
Fe_3O_4	Ferroferric oxide
Fe_3O_4@CSQ	Ferroferric oxide enwrapped by chitosan quaternary ammonium salt
Fe_3O_4@CSQ-PEG-PLGA	Fe_3O_4@CSQ double enwrapped by PEG-PLGA
CH_2Cl_2 (DCM)	Dichloromethane
B16	Melanoma cell
CCK	Cholecystokinin
TEM	Transmission Electron Microscopy
DLS	Dynamic Light Scattering
XRD	X-ray Diffraction
FTIR	Fourier Transform Infrared Spectra
PDI	Polydispersity index
EE	Encapsulate Efficiency
LC	Loading Content
ICP	Inductively Coupled Plasma
ICP-MS	Inductively Coupled Plasma Mass Spectrometry

1 Introduction

Magnetic resonance imaging (MRI) is widely used in clinical medical diagnosis, life science research, and other fields due to its non-invasive and multidimensional tomographic capabilities. It can realize the imaging of the structure, physiology, and chemical characteristics of tissues and organs *in vivo* [1-4]. Magnetic resonance imaging often needs to use contrast agent to shorten the imaging time and enhance the imaging of the lesion. The contrast agent can change the water proton's relaxation rate in the human body, enhance the clarity in the infection on the imaging contrast, and show the functional status of organs in the body. Therefore, it is a hot topic in the field of MRI to design and synthesize a safe, effective, and stable contrast agent, because development of new contrast agents is necessary to enhance the magnetic resonance imaging contrast in tissues of interest [5-8].

Recently, relatively safe ferroferric oxide (Fe_3O_4) has been studied as a contrast agent for signal enhancement as their low toxicity level compared to other commercial contrast agents. Fe_3O_4 nanoparticles have the quantum effect and large specific surface area, show superparamagnetism and magnetic tunneling effect, and have great potential applications in the field of biological engineering, such as cell therapy, tissue repair, drug delivery and magnetic resonance contrast agent [9-13]. In these requests, the surface of Fe_3O_4 nanoparticles must be

modified to enhance biocompatibility and to produce interactive functional groups on its particle surface with high magnetic saturation strength. The particle size of nano-scale should be distributed in 6-15 nm and can be excreted by the kidney in the form of rapid excretion from the body. Superparamagnetic Fe_3O_4 can show the magnetic effect under the action of the magnetic field, and there is no remanence after the magnetic field is canceled, so it has a good imaging effect [14-15].

Chitosan (CS) is the product of deacetylation of chitin and is a polysaccharide in nature. Chitosan has excellent biocompatibility, and biodegradability but no toxic side effects. Chitosan is lack of solubility in neutral or alkaline aqueous solution, so it is often cauterized to form ammonium salt to expand the scope of application of chitosan. Chitosan quaternary salt (CSQ) is a kind of cationic polymer electrolyte with an excellent hydrophilic group, which can be used in wastewater treatment, food processing, daily chemical production, drug loading and controlling, the preparation of antimicrobial materials, and other fields [16-18].

Co-precipitation method is the first method to the synthesis of Fe_3O_4 nanoparticles in a liquid phase. Precipitant (concentrated ammonia or sodium hydroxide solution) was added to ferric ions and ferrous ions solution. The solution of this multicomponent system can obtain Fe_3O_4 precipitation after precipitation reaction. The precipitate was then filtered, washed, and dried to obtain Fe_3O_4 nanoparticles with a size of 9-12 nm.

When Fe_3O_4 nanoparticles were prepared by this method, the agglomeration of nanoparticles was easy to occur during washing, filtering, and drying [19, 20].

The nanoparticles with CSQ as the surface ligand have strong positive charge and can agglomerate in the blood with more negative charge proteins, resulting in hemolysis, which is very dangerous to human body [21, 22].

Polylactic-co-glycolic acid (PLGA) is a copolymer of lactide acid (LA) and glycolide acid (GA), which is biocompatible and biodegradable. A large number of drug-containing controlled-release systems are used in the synthesis of biodegradable polymer materials. The nanoparticles prepared with PLGA as the carrier have the property of slow releasing rate, so it can decrease the number of drug delivery and dosage, enhance the targeting effect and pharmacodynamics, and thus have been widely used. Polyethylene glycol (PEG)-modified polylactic-co-glycolic acid (PEG-PLGA) can be utilized as the carrier material to prepare nanoparticles. Polyethylene glycol is a hydrophilic group, which can play a long cycle role. PEG-PLGA can be used as a drug-loaded drug delivery system. The nanoparticles preparation by multiple emulsion methods (w/o/w) are suitable for water-soluble drugs and can protect the activity of drugs. By adjusting the polymer concentration, the internal and external aqueous phase volume, stirring speed, concentration, and other

parameters can be obtained with better targeting and sustained release characteristics of nanoparticles [23-27].

Polyvinyl alcohol (PVA) is a polymeric emulsion stabilizer and dispersant which is soluble in water. The higher the water temperature is, the higher the solubility is, but it is almost insoluble in organic solvents. Due to the diversity of the copolymer structure, block copolymers with hydrophobic segments and hydrophilic segments form self-assembled micelles in a selective solvent, which has wide application prospects.

Polyether F68, the chemical composition of polyoxyethylene-polyoxypropylene block copolymers is commonly used as pharmaceutical excipients and emulsifiers. Water-soluble polyoxyethylene-polypropylene-polyoxyethylenetriblock copolymers [$(PEO)_x$–$(PPO)_y$–$(PEO)_x$], under the trade name Pluronics, are widely used as nonionic polymeric surfactants in medical and pharmaceutical fields and have been used to assist in the synthesis of nanostructures. In recent years, Pluronic copolymer as a drug carrier also has attracted wide attention [28-30].

In this research, the Fe_3O_4 nanoparticles (labeled as Fe_3O_4@CSQ) were prepared by encapsulation of quaternary ammonium salt of chitosan and encapsulated in PVA and F68 solution by amphiphilic (hydrophilic-Hydrophobic) micelle (PEG-PLGA). We developed the new method to functionalize the surface of Fe_3O_4 nanoparticles, which can

enhance the biosafety of Fe_3O_4 nanoparticles, to improve *in vivo* biosafety as contrast agents. The obtained magnetic Fe_3O_4@CSQ-PEG-PLGA were useful in process of contrast agent, thus, it seems to be a very promising material for application in advanced biotechnology and biomedicine.

2 Experiments

2.1 Materials

Chitosan quaternary ammonium salt was obtained from Sigma-Aldrich, China. PLGA-PEG copolymer with terminal carboxylic acid functional group (PLGA-PEG-COOH) was procured from Jinan Daigang Biomaterial Company. PVA and F68 were purchased from Sinopharm Chemical Reagent Co., Ltd. All other chemicals such as concentrated aqueous ammonia, concentrated hydrochloric acid, ferric chloride ($FeCl_3$), ferrous chloride ($FeCl_2$), CH_2Cl_2 (DCM) were reagent grade and used as such. The ultra-pure water used in the experimental sections has the conductivity of 18.25 megohm.

2.2 Synthesis of chitosan quaternary ammonium salt Fe_3O_4 nanoparticles

Fe_3O_4@CSQ nanoparticles were prepared using co-precipitation method. Synthesis experiments were conducted in a nitrogen atmosphere. Experimental apparatus is shown in figure 1.

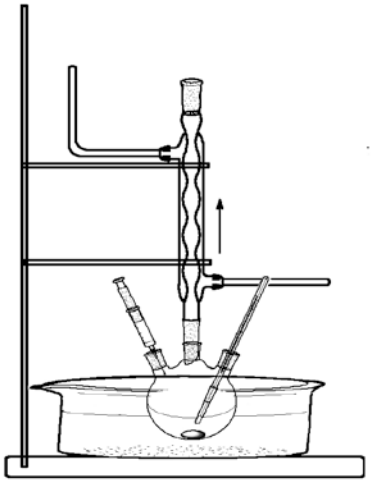

Fig. 1 Experimental apparatus

2.2.1 Dissolution of CSQ

CSQ was weighed and dissolved in 50 g pure water, and the CSQ solution was transferred to a three-necked flask (Note: there was a slight loss due to the viscosity of the solution and difficulty in transfer). Control the temperature of CSQ solution by using dimethyl silicone oil bath in 102 ^{o}C for 1 hour with cooling water poured into the condensed reflux, and continuous access to nitrogen out of oxygen (to avoid oxidation of ferrous iron ions).

2.2.2 Synthesis of nanosized Fe_3O_4 by co-precipitation method

0.1444 g of ferric chloride ($FeCl_3$) and 0.077 g of ferrous chloride ($FeCl_2$) were dissolved in 2 mL of concentrated hydrochloric acid, and the mixture of the above-prepared divalent and trivalent irons was added to the three-neck flask containing CSQ solution at 102 ^{o}C. Then 15 mL of concentrated ammonia water was added while maintaining a vigorous stirring. After reaction for 40 min under stirring, the cooled Fe_3O_4 colloid

was removed from the reaction apparatus. All the colloids were transferred to a dialysis bag by a pipette, placed on a magnetic stirrer, dialyzed in 4.5 L of water for three days seven times). Afterward, the coated nanoparticles were thoroughly washed with distilled water. The material was sealed and stored at 4 ^{o}C. Diagram of the preparation of Fe_3O_4@CSQ nanoparticles is shown in figure 2.

Reaction principle is as follows:

$$2Fe^{3+} + Fe^{2+} + 8OH^{-} \triangleq Fe_3O_4 + 4H_2O$$

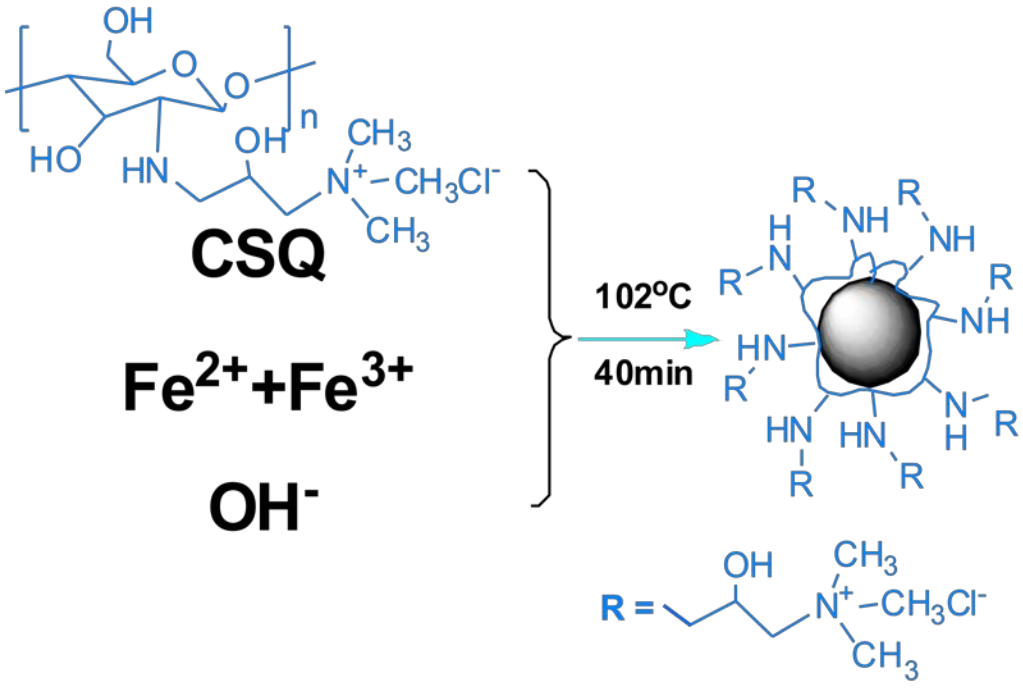

Fig. 2 Preparation of Fe_3O_4@CSQ nanoparticles

2.2.3 Fe_3O_4@CSQ nanoparticles encapsulated by double-emulsion methods

A schematic representation of the Fe_3O_4@CSQ nanoparticles encapsulated by the double emulsion process is shown in figure 3.

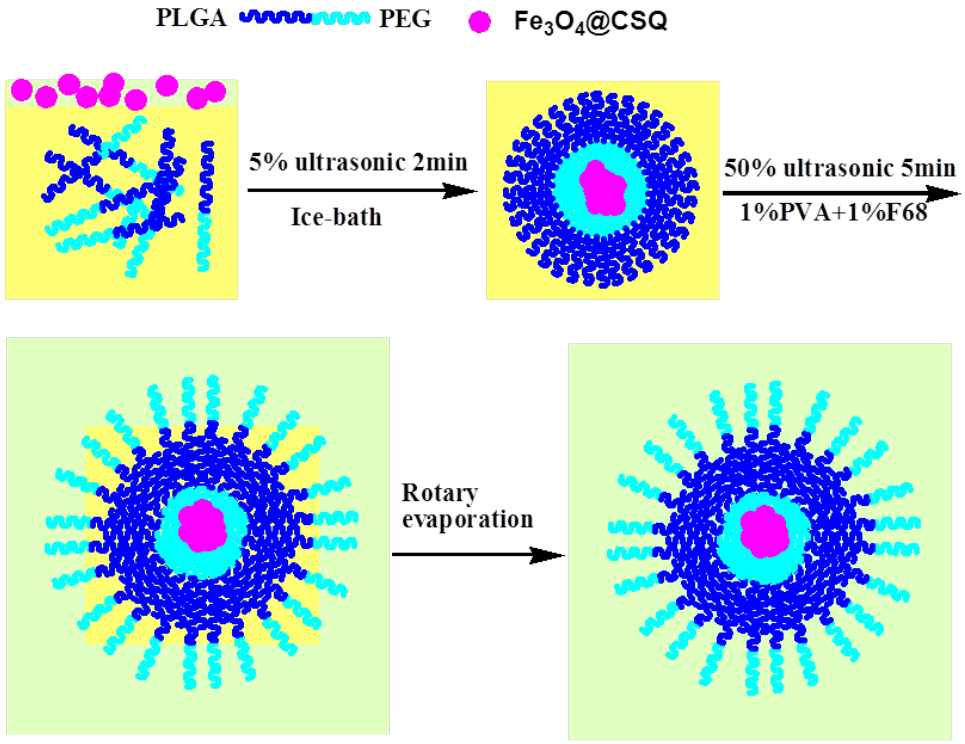

Fig. 3 Fe_3O_4@CSQ nanoparticles encapsulated by double emulsion method

Because the molecules in our emulsion process is big, we used a kind of surface active agent and emulsion stabilizer (solution of PVA and F68) to help with the emulsion process. The solution of PVA and F68 is prepared and the concentration is 1%.

The purified Fe_3O_4@CSQ nanoparticles were filtered through a 450 nm filter and the sample was concentrated to 20 mg/mL using an ultrafiltration tube. The sample was diluted by dilution. 200 μL of the 20 mg/mL sample contained 4 mg of Fe_3O_4@CSQ nanoparticles. The sample was denoted as 4.

As follows, 200 μL of the 20 mg/mL sample was added to 200 μL of

water, so 200 μL of this solution contains 2 mg of Fe_3O_4@CSQ nanoparticles, denoted as 2. In the same manner, use this kind of ratio dilution method to formulate solutions with different concentration: 4, 2, 1, 0.5, and 0.25. Then, PEG-PLGA 67.8 mg was dissolved in 6.78 mL DCM solution to make a 10 mg/mL solution. 1mL of this solution was added to six test tubes containing 0.25, 0.5, 1, 2, 4, five concentrations and 200 μL of tertiary water (blank control), respectively. In the first step of the emulsification, there is lots of oil but only little water. Under the effect of 50% power ultrasound for 5 minutes, the water is smashed into many tiny drops and dispersed in the oil, which contains PEG-PLGA, and because of the amphiphilic properties of PEG-PLGA, the hydrophilic group gradually spontaneously attaches to the Fe_3O_4@CSQ core and form the product of the first step of our emulsification. After we add the emulsion stabilizer PVA and F68, the system has a lot of water but relatively little oil. Under the effect of 50% power ultrasound for 5 minutes, in the same manner, the oil is smashed into tiny drops and dispersed in the water. As the oil drops contains the PEG-PLGA and the first-step product of the emulsification and because of the amphiphilic properties of the PEG-PLGA, the lipophilic groups can gradually attach to the inner part of the oil drops and therefore form the double-emulsified Fe_3O_4@CSQ nanoparticles.

The products were centrifuged at 1200 rpm for 10 min after rotary

evaporation, and each supernatant was dissolved in 1 mL of water. 50 μL of each sample was dissolved in 1 mL of water. The samples were washed with water and centrifuged repeatedly. After drying, Fe_3O_4@CSQ nanoparticles were entrapped to become Fe_3O_4@CSQ-PEG-PLGA.

2.3 Characterization of nanoparticles

Bright field transmission electron microscopic (TEM) images were obtained from with an FEITecnaiG2 microscope at an accelerating voltage of 200 kV.

Dynamic light scattering (DLS) (Zetasizer Nano series Nano-ZS, Malvern Instruments Ltd., Malvern, UK) was used to measure the hydrodynamic particle size.

Fourier transform infrared spectrometer (THERMO Scientific class-1 NICOLET FTIR-6700) was used to investigate the possible interaction of functional groups of coating with Fe_3O_4. The sample was mixed with KBr in proportion of 1:100 mg. The resolution of the spectra was set at 4 cm^{-1} with a scan average 30. The spectra were recorded in 500-4000 cm^{-1} wave number.

The properties of nanoparticles were measured by D/MAX-TTRIII (CBO) (Mac Science, Japan) X-ray diffractometer (XRD) for samples (D2 PHASER) which attached with Cu Ka radiation (k = 1.54060 A˚).

The relaxation measurements and material/cell magnetic resonance

images were performed on a 7.0 T small animal MRI instrument (BioSpec70/20USR), Bruker.

Absolute concentrations of Fe in each sample were measured by ICP-MS (PE8000, PerkinElmer, USA).

2.4 Cell experiment

To test the biosafety of the products, cell experiments were done, using B16 (melanoma cell). Cytotoxicity is the cell-cytotoxicity reaction after toxic materials are added. The experiment measures the viability of the cells after the nanoparticles are added. As the Fe_3O_4@CSQ-PEG-PLGA has biosafety theoretically, the cytotoxicity experiment is significant. In our cell experiment, the media is RSMI 1640 (penicillin-streptomycin and fetal bovine serum are added.). Trypsin Enzyme and PBS (phosphate buffer saline) are used during the passage process.

2.4.1 Incubation with cells

Add well-prepared B16 cell solution (6000 cells per milliliter) 100 μL to each holes (except the periphery 36 holes) of the 96-well plate. Put the 96-well plate into the incubator for 24 hours. Then, add Fe_3O_4@CSQ-PEG-PLGA and Fe_3O_4@CSQ solutions (i.e. 20 μg/mL, 10 μg/mL, 5 μg/mL, 0 μg/mL, respectively) to each hole of the 96-well plate. As there are 60 holes for the solutions, each solution with different concentration has 6 holes to be added. Then put the plate into the

incubator for another 24 hours.

2.4.2 Cell viability testing

10% CCK (cholecystokinin) of the RSMI 1640 media solution 200 μL was added to each hole of the plate and wait for 1 hour. As the CCK changed its color after it was added to cell solution, and the more the viability of cells is, the darker the solution is. Then we used microplate reader to determine the viability of the cells in each holes.

3 Results and discussion

3.1 Transmission electron microscopy analysis

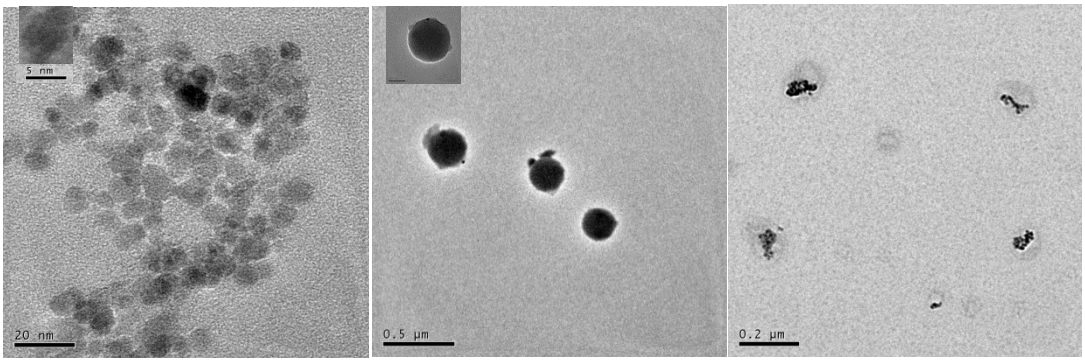

(a) Fe_3O_4@CSQ (b) PEG-PLGA (c) Fe_3O_4@CSQ-PEG-PLGA

Fig. 4 TEM images of Fe_3O_4@CSQ, PEG-PLGA, and Fe_3O_4@CSQ-PEG-PLGA

Figure 4 shows transmission electron microscopy (TEM) images of Fe_3O_4@CSQ, PEG-PLGA, and Fe_3O_4@CSQ-PEG-PLGA, respectively. From the TEM images of Fe_3O_4 nanoparticles shown in figure 4 (a), the prepared Fe_3O_4@CSQ nanoparticles are almost uniform in size. They are generally spherical in shape and about 9 nm in size, reaching to the sizes

of nanoparticles. The difference of the darkness is due to the overlapping of partial iron particles, which causes the density increase and electrons are hard to transmit. Figure 4 (b) is the PEG-PLGA double shell empty core particles. From figure 4 (c), the black part is the Fe_3O_4@CSQ particles and the white part is the PEG-PLGA. It can be seen that PEG-PLGA forms a uniform coating layer on the surface of the nanometer Fe_3O_4@CSQ particles, which increases the distance between the particles and keeps the Fe_3O_4@CSQ core dispersed in the product to maintain a smaller grain size. The core-shell structure of the magnetic composite particles is consistent with the theoretical prediction.

3.2 Particle size analysis of nanoparticles

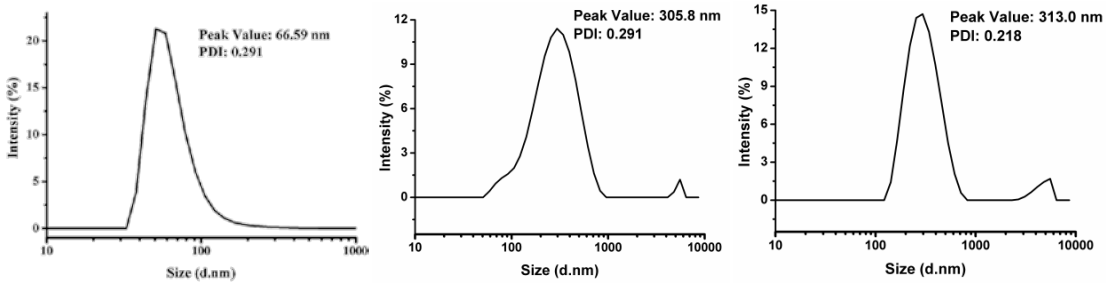

(a)Fe_3O_4@CSQ (b)PEG-PLGA (c)Fe_3O_4@CSQ-PEG-PLGA

Fig. 5 Particle size distribution curves

Figure 5 shows the particle size distribution of Fe_3O_4@CSQ, PEG-PLGA and Fe_3O_4@CSQ-PEG-PLGA particles, respectively. The data is the hydrodynamic particles size measured by DLS. In the figure, peak value is the major particle size in the measured particle. PDI is the polydispersity index, the lower the value, the more concentrated the data. The main particle size of Fe_3O_4@CSQ in figure 5 (a) is 66.6 nm,

and the main PEG-PLGA particle size in figure 5 (b) is about 305.8 nm. The main particle size of Fe_3O_4@CSQ-PEG-PLGA in figure 5 (c) is 313.0 nm. The size of the product observed in the TEM image was about 150 nm. This difference is due to the fact that the nanoparticles are completely swollen in the DLS aqueous phase, whereas TEM observes the size of the dried sample. PDI is equivalent to the standard deviation. When the PDI is below 0.3, we can say that the measured data are more concentrated. The results showed that the particle size of nanoparticles was small, and the PDI of the particles in the solution was low, indicating that the particle size of the nanoparticles was uniform.

3.3 Analysis of fourier transform infrared spectra

Figure 6 is the fourier transform infrared (FTIR) spectra of the polymers and the products before and after the double coating. It can be seen from the figure that the waveforms obtained at the part of the image are substantially coincident and not easily distinguishable. Therefore, when the data are tabulated, the infrared spectra obtained by Fe_3O_4@CSQ-PEG-PLGA are shifted upward to separate them easy to compare. The red lines (coated particles) at 565 cm^{-1} relative to the black line (drug) has a new peak shape, which is the characteristic peaks created by Fe-O bond of Fe_3O_4 under the effect of infrared ray, indicating that the reaction products containing Fe_3O_4, and verify the coating

success. Other peak shape analysis: asymmetric stretching vibration of C-O-C at 1082 cm^{-1} is the characteristic peak in PEG; C=O stretching vibration peak at 1750 cm^{-1} is the characteristic peak in PLGA; 3250 cm^{-1} is the N-H peak in the chitosan, but is not obvious because most of the nitrogen atoms associate with ferroferric oxide.

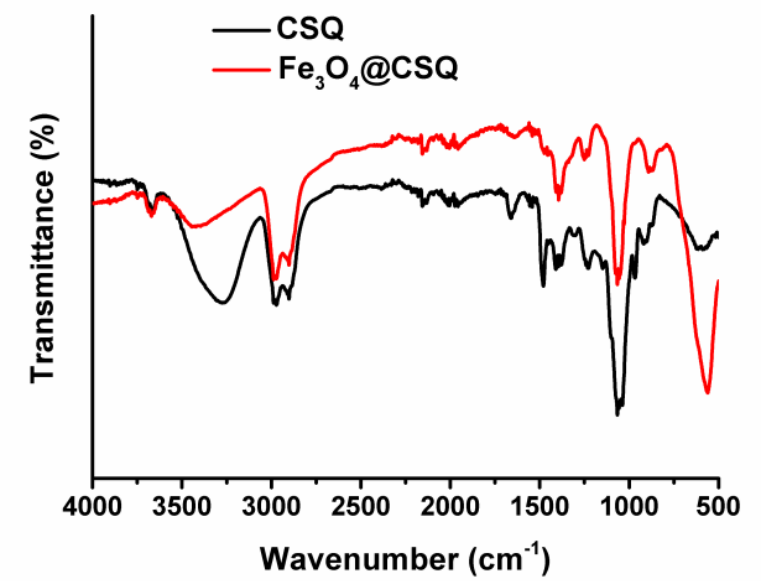

(a) CSQ and Fe_3O_4@CSQ

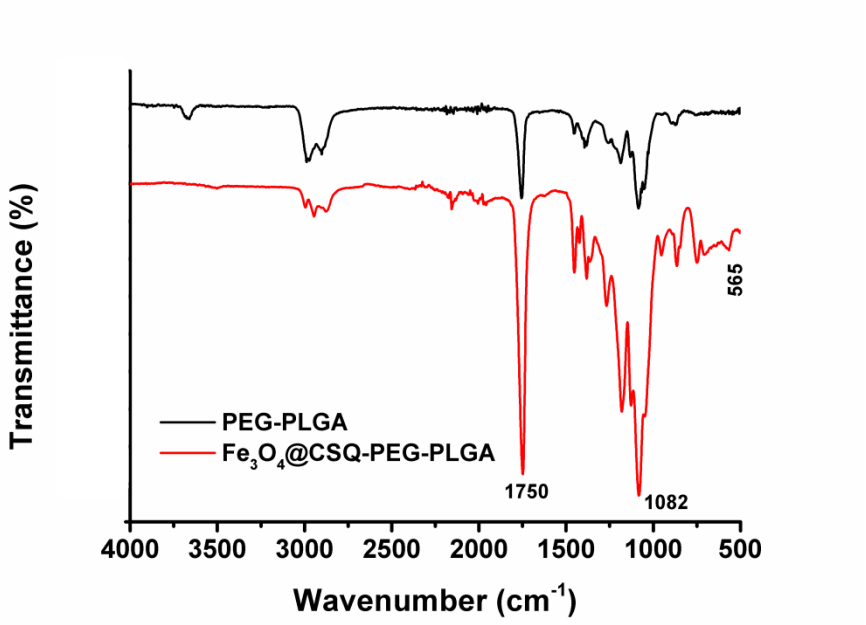

(b) PEG-PLGA and Fe_3O_4@CSQ-PEG-PLGA

Fig. 6 FTIR spectra of the polymers and the products

3.4 X-ray diffraction analysis

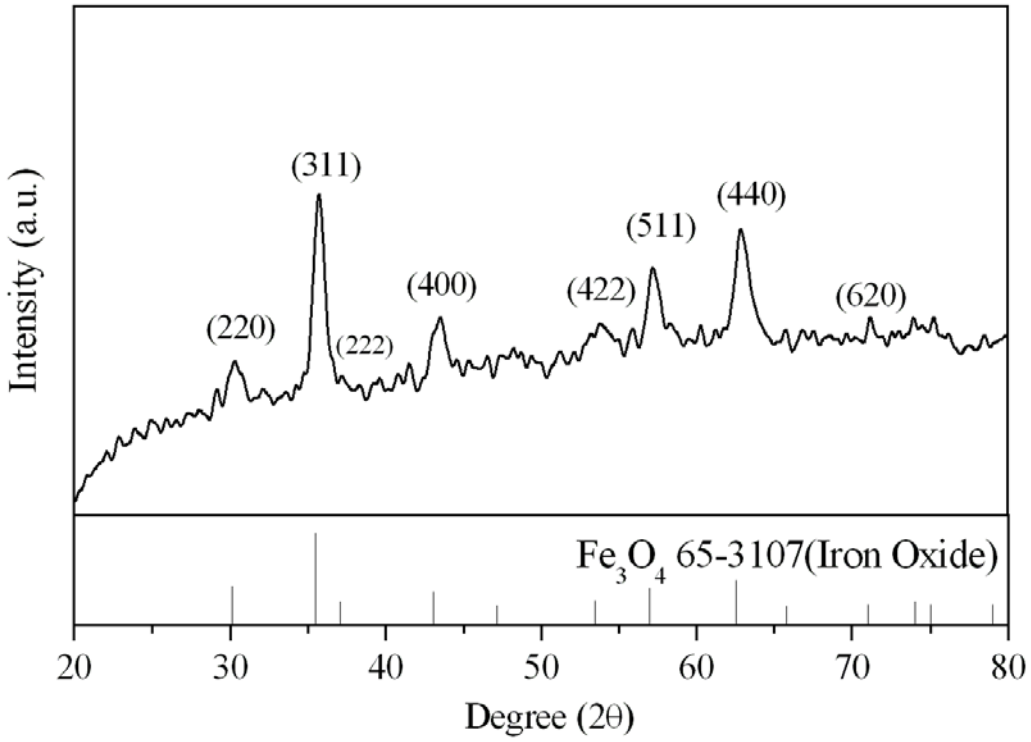

Fig. 7 X-ray diffraction of the synthesized Fe_3O_4

Figure 7 shows the X-ray diffraction (XRD) data of the synthesized Fe_3O_4. As shown, the 6 characteristic peaks are obtained by XRD. (220), (311), (222), (400), (422), (511), (440) and (620) are corresponding to the crystal face of Fe_3O_4 lattice, respectively. These peaks are the characteristic peak shapes exhibited by the Fe_3O_4 trans-spinel crystal structure. The results showed that Fe_3O_4 has been successfully prepared after the reaction between $FeCl_3$ and $FeCl_2$ by comparison with JCPDS standard card.

3.5 Analysis of hysteresis loop

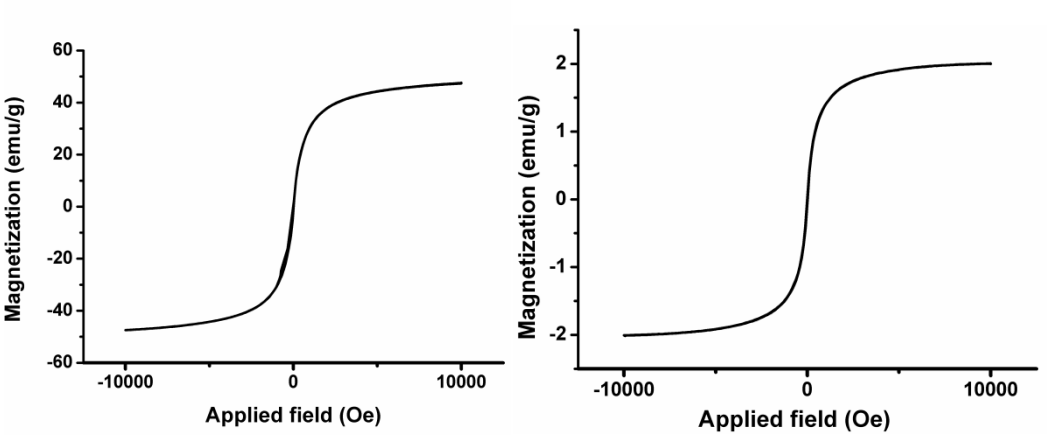

(a)Fe_3O_4@CSQ (b)Fe_3O_4@CSQ-PEG-PLGA

Fig. 8 Hysteresis loops of Fe_3O_4@CSQ and Fe_3O_4@CSQ-PEG-PLGA

Fig. 8 shows the hysteresis loops of Fe_3O_4@CSQ and Fe_3O_4@CSQ-PEG-PLGA, respectively. In general, the magnetization of a magnetic material increases with the increase of the external magnetic field, and eventually reaches saturation. When the external magnetic field is canceled, the magnetization of the magnetic object cannot be reduced to zero. This indicates that the change of its magnetization intensity lags behind the change of the external magnetic field intensity. This phenomenon is called hysteresis. The coincidence of the three hysteresis loops indicates that the coercivity is zero, indicating that the sample has superparamagnetism, so it is good for imaging and stabilizing of the particles. When the size of the magnetic particles is smaller than that of the magnetic monolithic size (20-50 nm), the particles can show great magnetism under a weak external magnetic field and after the external magnetic field is revoked, the remnant magnetism is zero. And the value

of the rear ordinate Hm of the coating becomes small, indicating that the coated particles are dispersed and the interaction of particles magnetic fields is weakened.

3.6 Analysis of zeta potential

The Fe_3O_4@CSQ particles are positively charged due to the CSQ shell. The human body contains many negatively charged substances. Therefore, Fe_3O_4@CSQ particles have two problems to be used as contrast agent: (1) the Fe_3O_4@CSQ is positively charged so it is easy to agglomerate with the negatively charged proteins in human body, resulting in hemolysis, which is harmful to human body. (2) It doesn't have long enough circulation in human body, resulting in an suboptimal imaging.

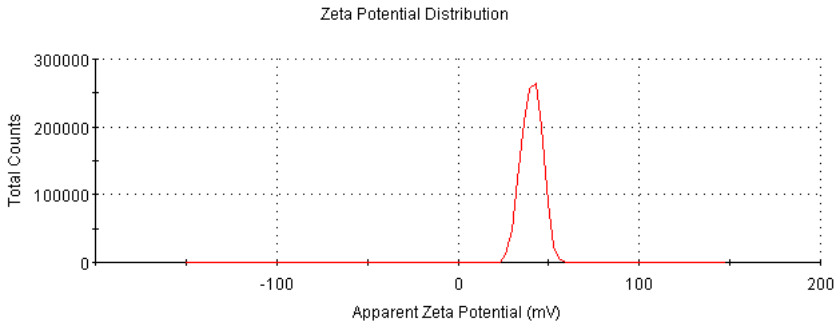

(a)Fe_3O_4@CSQ

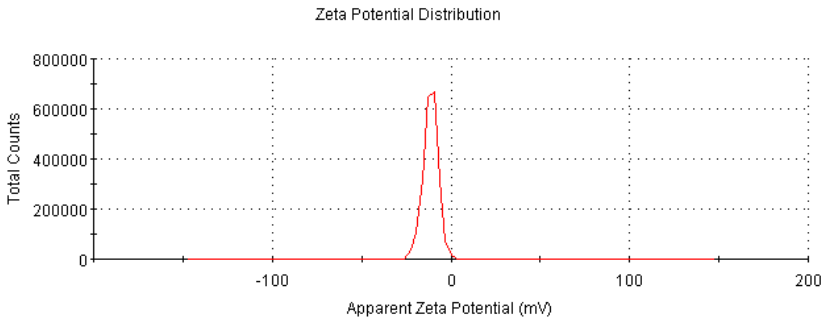

(b)Fe_3O_4@CSQ-PEG-PLGA

Fig. 9 Zeta potential

Figure 9 (a) and (b) show the zeta potentials of Fe_3O_4@CSQ and Fe_3O_4@CSQ-PEG-PLGA, respectively. The data in the picture shows that after the Fe_3O_4@CSQ nanoparticles are coated by PEG-PLGA, the potential becomes negative. It avoids the hemolysis and increases the biosafety. Besides, the negatively charged nanoparticles and the electronegative proteins repel each other so they are more stable *in vivo* existence.

3.7 Analysis of relaxation rate

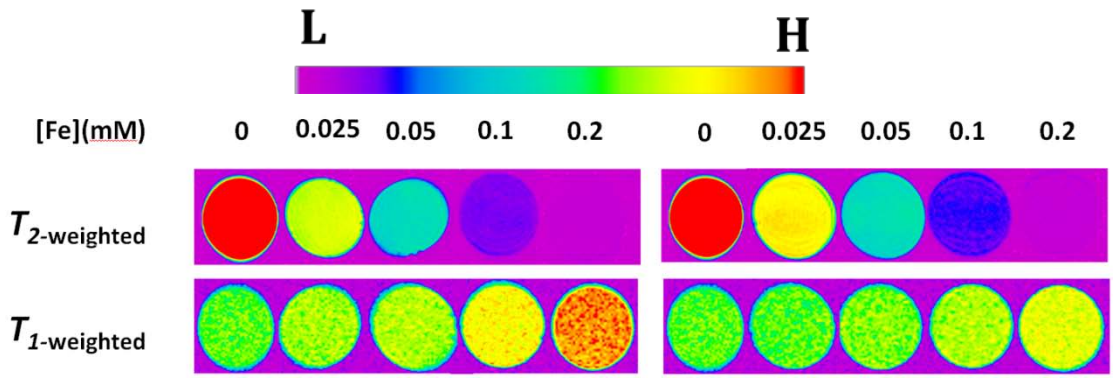

Fig. 10 The relaxation rate of MRI-T_2 and MRI-T_1

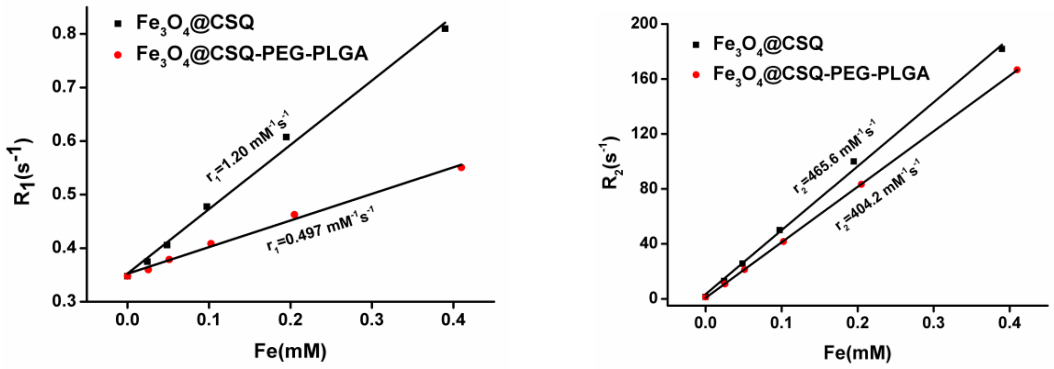

Fig. 11 The relaxation rate of Fe_3O_4@CSQ and Fe_3O_4@CSQ-PEG-PLGA

Fig. 10 is the relaxation rate of MRI-T_1 (longitudinal relaxation time of magnetic resonance) and the relaxation rate of MRI-T_2 (transverse relaxation time of magnetic resonance). Relaxation is an inherent property of nature; any system has the property of returning to the original (original, equilibrium) state after the external stimulus is withdrawn; this process of returning from the excited state to the equilibrium state is the relaxation process. Proton can be excited by the pulse magnetic fields; just like from the ground state goes into the excited state. The pulse magnetic field is a transient magnetic field, so the proton will gradually return to the ground state after the pulse magnetic field disappears. The time used from the ground state back to the excited state is the relaxation time. The iron nanoparticles have great magnetism under the pulsed magnetic field after their enrichment at the lesion site. The magnetic field will act on the hydrogen proton of the lesion site and make the relaxation time shorten, and differences in time with other parts of the iron nanoparticles are distinguished from other parts of the image.

The longitudinal recovery time T_1 is due to the excitation of the antiparallel to the static magnetic field proton back to parallel state, so the longitudinal magnetization time increases. The relaxation rate follows an exponential law. The time required to increase the T_1 intensity from 0 to 63% of the maximum value is defined as the longitudinal relaxation time (T_1). The shorter the time is, the stronger the signal is. The production of

lateral recovery time T_2 is due to the phase synchronization proton becoming non-synchronous, so the lateral magnetization is reduced. The relaxation time follows the exponential decay law, and the time used to decrease T_2 intensity from maximum to 37% of maximum is defined as the transverse relaxation time (T_2). The shorter the time is, the stronger the negative signal is, the darker the image.

The slopes in figure 11 represent the relaxation rate of Fe_3O_4@CSQ and the relaxation rate of the coated Fe_3O_4@CSQ-PEG-PLGA, respectively.

The relaxation rate is the reciprocal of the relaxation time. The higher the relaxation rate, the shorter the relaxation time, and the higher the sensitivity of the nanoparticles it is to detect lesions. The difference of relaxation time T_1 and T_2 between human normal tissue and lesion tissue is an important parameter of MRI technique. The effect of the contrast agent is to change the proton spin relaxation of the lesion site to image. T_1 values are generally 10^2-10^4 milliseconds, T_2 value is generally 10-100 ms. Therefore, compared with T_1 contrast agent, superparamagnetic T_2 contrast agent can be more effective in improving the surrounding water proton relaxation rate, having a better imaging effect and longer time in vivo circulation. When the surface of iron particles are coated with PEG-PLGA, the distance of water molecules from the relaxation center becomes slightly larger, so the coating has a slight impact on the imaging sensitivity. As can be seen, after coating, R_1 significantly decreased, but

R_2 decreased significantly. Therefore, the particles as T_2 contrast agent sensitivity is still high, as T_1 contrast agent sensitivity decreased. According to the color bar chart, when the iron content increases, T_1 positive imaging effect and T_2 negative imaging results are enhanced.

3.8 Determination of entrapment efficiency and loading content

Figure 12 shows the relationship between Fe_3O_4 encapsulate efficiency (EE) and loading content (LC) and the ratio of Fe_3O_4 to PEG-PLGA measured by ICP-MS. EE is the ratio of the amount of iron on the encapsulated particles to the total amount of iron, and LC is the ratio of the amount of iron on the encapsulated particles to the total amount of the product.

$$\mathrm{EE} = \frac{\mathrm{M(iron\ on\ the\ encapsulated\ particles)}}{\mathrm{M(total\ amount\ of\ iron)}} \times 100\%$$

$$\mathrm{LC} = \frac{\mathrm{M(iron\ on\ the\ encapsulated\ particles)}}{\mathrm{M(\ total\ amount\ of\ the\ product)}} \times 100\%$$

After the PEG-PLGA was encapsulated by double emulsion method, the emulsion was centrifuged and the supernatant liquid was taken. The supernatant was subjected to nitrification. In this case, all the organic matter in the supernatant is decomposed and Fe is present in the form of Fe^{3+}. ICP-MS can accurately determine the concentration of trace ions. Then the concentration of iron ions in the supernatant liquid can be

obtained and used to calculate EE and LC. It can be seen that when the ratio is 0.018, the utilization ratio and loading rate can reach relatively high level, so when the ratio is 0.018, the coating efficiency is the highest.

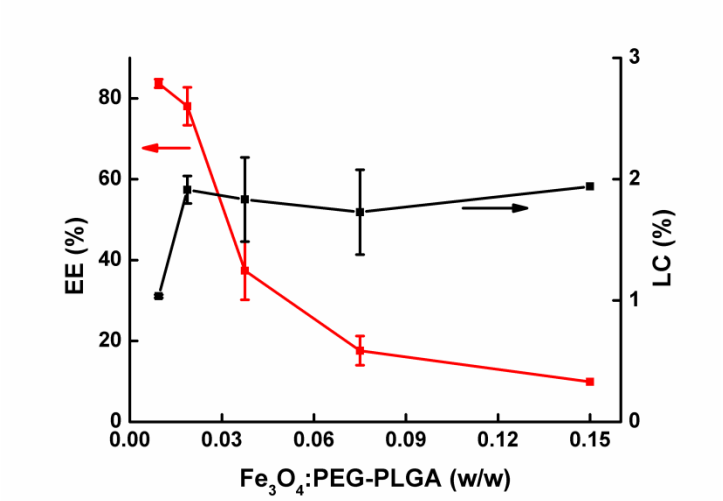

Fig. 12 The relationship between Fe_3O_4 encapsulate efficiency (EE) and loading content (LC) and the ratio of Fe_3O_4 to PEG-PLGA

3.9 Cell experiments results

The cell viability data by the micro plate reader test is shown figure 13. According to the results, the Fe_3O_4@CSQ can significantly influence the viability of the B16 cell but the Fe_3O_4@CSQ-PEG-PLGA can attenuate the cytotoxicity of the iron particles.

In the first graph, cell keep alive though the concentration of Fe_3O_4@CSQ-PEG-PLGA increase. In the second graph, cell viability decreased significantly with the increase of concentration Fe_3O_4@CSQ since the positive charge of CSQ can cause the damage to the cell membrane.

In conclusion, the Fe_3O_4@CSQ-PEG-PLGA has improved biocompatibility.

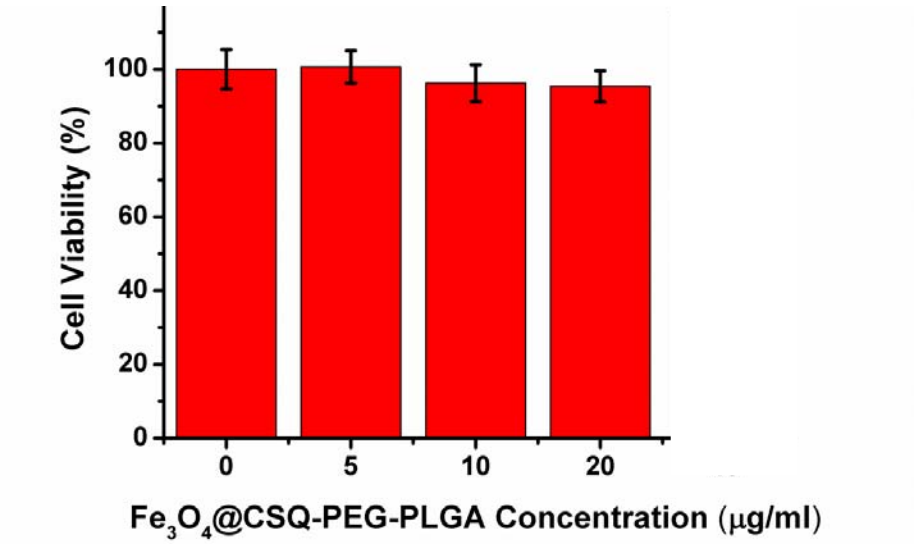

(a)

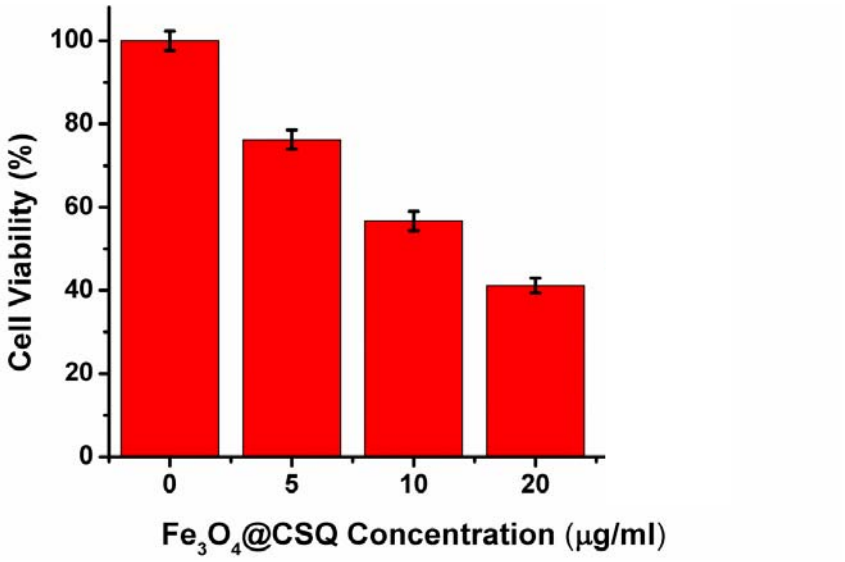

(b)

Fig. 13 Cell viability of Fe_3O_4@CSQ-PEG-PLGA (a) and Fe_3O_4@CSQ (b)

4 Conclusion

Nanoparticles of Fe_3O_4 were firstly prepared by encapsulation with CSQ

and then, using double-emulsion method, were encapsulated twice by polymer amphiphilic (hydrophilic-hydrophobic) micelles PEG-PLGA to obtain Fe_3O_4@CSQ-PEG-PLGA nanoparticles. Transmission electron microscopy observation and particle size analysis showed that the surface of the Fe_3O_4@CSQ core was dispersed in the product by the encapsulation of PEG-PLGA, and the result is consistent with the core-shell structure theory. FTIR spectra and X-ray diffraction characterization confirmed the existence of Fe_3O_4 in the nanoparticles.

The results show that the particle size of Fe_3O_4@CSQ-PEG-PLGA nanoparticles is small, and the zeta potential of zeta potential is negative to avoid aggregation with the proteins in the blood, having little harm to the human body but high biological safety and long circulating time. Meanwhile, the nanoparticles show superparamagnetism and high relaxation rate，so it can be can be concluded that the contrast effect of the nanoparticles is good. The results of determination of entrapment efficiency and loading content show that when the mass ratio of Fe_3O_4 to PEG-PLGA is 0.018, the coating efficiency is the highest.

Cell toxicity experiment show that the Fe_3O_4@CSQ-PEG-PLGA nanoparticles could improve the biosafety of the Fe_3O_4@CSQ and have no toxic side effect on the cells proliferations, and the biosafety is very high. Therefore, the Fe_3O_4@CSQ-PEG-PLGA nanoparticles can be used as a safe, stable and effective new MRI-T_2 contrast agent.

References

1. Srivastava AK, Kadayakkara DK, Bar-Shir A, Gilad AA, McMahon MT, Bulte JWM (2015) Advances in using MRI probes and sensors for *in vivo* cell tracking as applied to regenerative medicine. Dis Mod Mech 8:323-336
2. Airan RD, Li N, Gilad AA, Pelled G (2013) Genetic tools to manipulate MRI contrast. NMR Biomed 26:803-809
3. Stephen ZR, Kievit FM, Zhang M (2011) Magnetite nanoparticles for medical MR imaging. Mater Today 7-8:330-338
4. Zhang L, Wang Y, Tang YH, Xie CY, Zhang HJ, Gu P, Wei XB, Yang GY, Gu HC, Zhang CF (2013) High MRI performance fluorescent mesoporous silica-coated magnetic nanoparticles for tracking neural progenitor cells in an ischemic mouse model. Nanoscale 5:4506-4516
5. Gao JH, Liang GL, Cheung JS, Pan Y, Kuang Y, Zhao F, Zhang B, Zhang XX, Wu EX, Xu B (2008) Multifunctional yolk-shell nanoparticles: A potential MRI contract and anticancer agent. J Am Chem Soc 130(35):11828-11833
6. Laurent S, Forge D, Port M, Roch A, Robic C, Vander E, Muller R (2008) Magnetic iron oxide nanoparticles: synthesis, stabilization, vectorization, physicochemical characterizations, and biological applications. Chem Rev 108:2064-2110
7. Sulek S, Mammadov B, Mahcicek DI, Sozeri H, Atalar E, Tekinay AB, Guler MO (2011) Peptide functionalized superparamagnetic iron oxide nanoparticles as MRI contrast agents. J Mater Chem, 21:15157-15162
8. Gupta AK, Gupta M (2005) Synthesis and surface engineering of iron oxide nanoparticles for biomedical applications. Biomaterials 26:3996-4021
9. Yang G, Zhang BL, Wang J, Wang M, Xie SB, Li X (2016) Synthesis and characterization of poly(lactic acid)-modified superparamagnetic iron oxide nanoparticles. J SOL-GEL Sci Techn 77:335-341

10. Salgueirino-Maceira V, Correa-Duarte M A (2016) Increasing the complexity of magnetic core/shell structured nanoparticles for biological applications. Advanced Materials 19(23):4131-4144
11. You CC, Chompoosor A, Rotello VM (2016) The biomacromolecules nanoparticle interface. Nano Today 2:34-43
12. Zhang L, Wang Y, Tang YH, Jiao Z, Xie CY, Zhang HJ, Gu P, Wei XB (2013) High MRI performance fluorescent mesoporous silica-coated magnetic nanoparticles for tracking neural progenitor cells in an ischemic mouse model. Nanoscale 5:4506-4516
13. Dai FY, Du MH, Liu YG, Liu GY, Liu QJ, Zhang X (2014) Folic acid-conjugated glucose and dextran coated iron oxide nanoparticles as MRI contrast agents for diagnosis and treatment response of rheumatoid arthritis. J Mater Chem B: 2240-2247
14. Matsumoto Y, Jasanoff A (2008) T-2 relaxation induced by clusters of superparamagnetic nanoparticles: Monte Carlo simulations. Magn Reson Imaging 26:994-998
15. De M, Chou SS, Joshi HM, Dravid VP (2011) Hybrid magnetic nanostructures (MNS) for magnetic resonance imaging applications. Adv Drug Deliver Rev 63:1282-1299
16. Li R, Li P, Cai J, Xiao SJ, Yang H, Li AM (2016) Efficient adsorption of both methyl orange and chromium from their aqueous mixtures using a quaternary ammonium salt modified chitosan magnetic composite adsorbent. Chemosphere 154:310-318
17. Zhang CL, Hu XM, Ying SY, Wang F (2013) Preparation of magnetic quaternary chitosan salt and its adsorption of methyl orange from water. Huanjingkexue, 34:1815-1821
18. Li SD, Li PW, Yang ZM (2014) Synthesis and characterization of chitosan

quaternary ammonium salt and its application as drug carrier for ribavirin. Drug Delivery 21:548-552

19. Lee MS, Su CM, Yeh JC, Wu PR, Tsai TY, Lou SL (2016) Synthesis of composite magnetic nanoparticles Fe_3O_4 with alendronate for osteoporosis treatment. Int J Nanomed 11:4583-4594
20. Wang YM, Cao X, Liu GH, Hong RY, Chen YM, Chen XF, Li HZ, Xu B, Wei, DG (2011) Synthesis of Fe_3O_4 magnetic fluid used for magnetic resonance imaging and hyperthermia. J Magn Magn Mater 323:2953-2959
21. Mahmoudi M, Simchi A, Milani AS, Stroeve, P (2009) Cell toxicity of superparamagnetic iron oxide nanoparticles. J Colloid Interface Sci 336:510-518
22. Ziegler-Borowska M, Chełminiak D, Sio´dmiak T, Sikora A, Marszałł MP, KaczmarekH(2014)Synthesis of chitosan coated magnetic nanoparticles with surface modified with long-distanced amino groups as a bioligands carrier. Mater Lett. 132:53-65.
23. DanhierFabienne, Ansorena Eduardo, Silva Joana M (2012) PLGA-based nanoparticles: An overview of biomedical applications. J Control Release 161:505-522
24. Cao LB, Zeng S, Zhao W (2016) Highly stable PEGylatedpoly (lactic-co-glycolic acid) (PLGA) nanoparticles for the effective delivery of docetaxel in prostate cancers. Nanoscale Res Lett 11:305
25. Hu SY (2010) Endostar loaded PEG-PLGA nanopartieles: In vitro and in vivo evaluation. Inter J Nanomed 24(5):1039-1048.
26. Qi F, Wu J, Hao DX, Yang TY, Ren Y, Ma GH, Su ZG (2014) Comparative Studies on the Influences of Primary Emulsion Preparation on Properties of Uniform-Sized Exenatide-Loaded PLGA Microspheres. Pharm Res 31(6): 1566-1574
27. Ahn JH, Park EJ, Lee HS, Lee KC, Na DH (2011) Reversible blocking of amino

groups of octreotide for the inhibition of formation of acylated peptide impurities in poly(lactide-co-glycolide) delivery systems. Aaps Pharmscitech. 12(4):1220-1226

28. Adams ML, Lavasanifar A, Kwon GS (2003) Amphiphilic block copolymers for drug delivery. J Pharm Sci 92(7): 1343-1355
29. Batrakova EV, Kabanov, AV (2008) Pluronic block copolymers: Evolution of drug delivery concept from inert nanocarriers to biological response modifiers. J Control Release130(2):98-106
30. Sezgin Z, Yuksel N, Baykara T (2007) Investigation of pluronic and PEG-PE micelles as carriers of meso-tetraphenylporphine for oral administration. Int J Pharm 332:161-167

Acknowledgments

In the research, authors got great support of Professor Chen Chunying from the research group in the National Center for Nanoscience and Technology. Thanks to Dr. Zhou Huige who taught us to master the basic research techniques and the use of large-scale equipment, so we can complete our experiments successfully. Our research team members thank to the teacher Chen with the lofty respect and wish heartfelt thanks!

Resumes of the team members and instructor

Wang Shengzhuo is a student of Class 12 Grade 12 at Tsinghua University High School. He has strong interest in chemistry and won the Beijing Olympic Chemistry Competition First Prize for two consecutive years, National talent show in Mathematics, Chemistry, and Physics First Prize in chemistry, American Mathematics Competition (12) top 5%. Meanwhile, he is the Tsinghua University High School debate team captain, lead tenor of Tsinghua University High School Chorus.

Hu Chenxu is a student of Class 10 Grade 12 at Tsinghua University High School. He studies hard and always has excellent academic performance. His performances on tests are always among the best of students. Meanwhile, he has strong interest in chemistry and won the National Olympic Chemistry competition second prize and the Beijing Olympic Chemistry Competition first prize. He is also good at physics and won the National Olympic Physics Competition second prize.

Yu Shixing is a student of Class 10 Grade 12 at Tsinghua University High School. He has strong interest in chemistry and won second prize in the Preliminary Chinese Olympic Chemistry Competition for two consecutive years.

Chen Xinfu is a chemistry teacher of Tsinghua University High School.